A novel fouling control strategy for forward osmosis membrane during sludge thickening via self-forming protective layer

Xiawen Yi[a], Kang Chen[b], Ming Xie[c], Pin Zhao[a], Weilong Song[a], Xinhua Wang[a,d,*]

[a] Jiangsu Key Laboratory of Anaerobic Biotechnology, School of Environmental and Civil Engineering, Jiangnan University, Wuxi 214122, PR China

[b] Jiangsu Nollet Intelligent Water Equipment Co. Ltd, Nantong 226331, PR China

[c] Department of Chemical Engineering, University of Bath, Bath, BA2 7AY, UK

[d] Jiangsu Collaborative Innovation Center of Technology and Material of Water Treatment, Suzhou University of Science and Technology, Suzhou 215009, PR China

[*] Corresponding author: Tel: +86-510-85910765, E-mail: xhwang@jiangnan.edu.cn (X. Wang).

Abstract

Severe forward osmosis (FO) membrane fouling significantly limited the application of FO membrane for sludge thickening. Here, a novel antifouling strategy by loading a self-forming protective layer on FO membrane surface was proposed in this study. The protective layer was coated on the FO membrane surface not with any chemicals but via a short-term operation of FO process with activated sludge as feed solution. Results indicated that the self-forming protective layer had no negative effect on membrane intrinsic properties, whereas the presence of protective layer made the FO membrane surface more hydrophilic and more negatively charged. Compared with the control FO (C-FO) membrane, the modified FO (M-FO) membrane with a protective layer showed a better sludge thickening efficiency and a lower flux decline during sludge thickening. In addition, less deposited foulants and a better fouling reversibility were observed for the M-FO membrane after two cycles of sludge thickening, implying that the protective layer effectively mitigated the FO membrane fouling during sludge thickening. This phenomenon could be explained from two aspects. Firstly, the protective layer apparently could improved the hydrophilicity and negative charge of the membrane surface, which effectively slowed downprevent the deposition of subsequent organic matter and microorganisms. In addition, the loose protective layer had an excellent support barrier effect, which not only avoided the mutual extrusion of subsequent foulants but also alleviated the deposition of irreversible foulants within membrane matrix. Our finding is helpful for better shed light on understanding FO membrane fouling and developing novel mitigation strategies via a fouling protective layer at an excessive highfouling propensity matrix with high sludge concentration. and for developing the fouling strategy via a fouling protective layer.

Keywords: forward osmosis; membrane fouling; fouling control; protective layer; sludge treatment

1. Introduction

As an economical and efficient process, activated sludge process (ASP) has been widely applied in wastewater treatment plants (WWTPs) [1,2]. However, waste activated sludge (WAS), a by-product of the ASP, is becoming one ~~of the inevitable~~grand challenge~~s~~ to the WWTPs ~~and local government~~ with ~~the~~ rapid industrialization and urbanization [3]. For example, ~~A~~according to the Statistical Yearbook of Urban and Rural Construction in China, the annual WAS production had risen to 13.3 million tons dry solids in 2020 [4]. If not being appropriately managed, such a large amount of WAS would cause serious secondary pollution in the ~~worldwide~~ environment [5]. Except for a large production of WAS, its treatment cost was so high that equivalent to wastewater treatment [6-8]. Based on the large output and high treatment cost of WAS, the treatment and disposal of WAS have aroused increasingly interests.

Sludge thickening is a vital step of sludge treatment and disposal, which can effectively minimize the volume of WAS, cut down the treatment cost of subsequent transportation and disposal, and lighten the environmental burden [9,10]. Currently, membrane separation technology including microfiltration (MF), ultrafiltration (UF) and forward osmosis (FO) has emerged as an effective technology for thickening WAS owing to a less footprint, a higher thickening efficiency and a better effluent water quality [6,7,11-19]. Compared to the MF and UF membrane, FO membrane is more suitable for thickening WAS due to its higher rejection capability, superior water flux stability against fouling and less energy consumption [20-24]. Although obvious advantages have shown in using FO membrane for sludge thickening (FST), there are still some challenges including salinity build-up and membrane fouling limiting sludge thickening efficiency. In order to mitigate salinity

build-up, Yi et al. (2021) utilized MF membrane to discharge soluble salt in the FST process, which successfully alleviated the salinity build-up and notably enhanced the sludge thickening efficiency [7]. In this case, membrane fouling resulting in an obvious flux decline of FO membrane becomes a major bottleneck of the FST process. According to previous literature on the FST process [6,7, 25,26], sludge concentration had a significant impact on FO membrane fouling, and MLSS concentration of 30 g/L was a turning point of FO membrane fouling, i.e., the membrane fouling became dramatical severe when MLSS concentration was more than 30 g/L. Besides that, organic fouling and biofouling were the main type of FO membrane fouling, and aromatic and hydrophilic organic matters controlled the fouling behavior during sludge thickening. Furthermore, according to Yi et al. (2022), the development of FO membrane fouling during sludge deep thickening could be divided into three stages, i.e., sand-like fouling stage, loose fouling layer stage and dense fouling layer stage [26]. Except for analyzing fouling behaviors of FO membrane, only a few researchers have proposed some methods to alleviate FO membrane fouling during sludge thickening. For instance, Sun et al. (2019) proposed adding poly-aluminum chloride into WAS to alleviate FO membrane fouling by changing the properties of WAS [27], and Ng et al. (2019) prepared a novel three-layer FO membrane to alleviate membrane fouling by improving the anti-fouling performance of FO membrane [28]. Nevertheless, there is no doubt that adding chemicals increase the treatment cost and membrane modification is a complex and expensive process. Therefore, it is essential to explore a novel fouling control method for FO membrane during sludge thickening.

Currently, FO membrane fouling is mitigated by three pathways including regulating the properties of feed solution, optimizing operating conditions, and modifying the surface of membrane [29]. Compared to the other ones, membrane surface modification is a fundamental but most

effective method. Whereas, most of the modifications are difficult and complicated, and chemical modification will consume a lot of chemicals and even cause the release of hazardous waste [30]. In this case, a novel membrane fouling strategy via coating a protective layer on the membrane surface has been proposed in recent years [30-34]. Specifically, the protective layer composed of chemical substance is coated on the membrane surface through electrostatic adsorption, hydrogen bonding, covalent bonds and other interactions, and the protective layer can be decoated by chemical agents after membrane fouling, meaning that the fouling layer deposited on the protective layer is removed at the same time. After that, a new protective layer is coated on the membrane surface again with the same coating method. Although the coating-decoating-recoating strategy had a good effect on mitigating membrane fouling, the process needs chemical reagents for coating and decoating protective layer, resulting in an increase in the cost and potential risk of environment [30].

Inspiring by the successful concept of building a protective layer for mitigating membrane fouling, a novel self-forming protective layer for mitigating FO membrane fouling during sludge thickening was prepared in this study. Compared with previous literature applying chemical reagents for coating and decoating protective layer, the self-forming protective layer was coated on the FO membrane surface via activated sludge and was removed by physical cleaning, implying a more easy and environmental-friendly process. So far, studies on using a self-forming protective layer for mitigating membrane fouling have not been found in current literature. Thus, the aims of current study are to investigate the feasibility of using the self-forming protective layer to mitigate membrane fouling, and to evaluate the long-term performance of FO membrane with a self-forming protective layer during sludge thickening.

2. Materials and methods

2.1 Reactor and sludge characteristics

Two identical laboratory-scale reactors with an effective volume of 3.8 L were operated in parallel for thickening WAS (as illustrated in Fig. S1). The WAS was directly collected from a local wastewater treatment plant (Wuxi Xincheng WWTP), and its characteristics were summarized in Table S1. Details of the reactor have been reported in our previous literature [7,26]. Briefly, the reactor consisted of an MF and an FO membrane module with an effective area of 0.032 m^2 and 0.024 m^2, respectively. The MF membrane (made of polyvinylidene fluoride (PVDF), supplied by Zizheng Environment Inc., China) with a nominal pore size of 0.20 μm was continuously operated under the mode of stable flux, and its water flux was maintained at approximately 2.3 LMH by a peristaltic pump. The FO membrane was made of cellulose triacetate (CTA) (Fluid Technology Solutions Inc., United States) and its active layer faced with the WAS (AL-FS mode). The driving force of FO membrane was supplied by the draw solution of 1 M NaCl solution, and a conductivity control system was applied for maintaining a stable draw solution concentration. In order to mitigate membrane fouling and maintain the dissolved oxygen concentration in the mixed liquors, aeration was introduced with an aeration rate of 200 L/min. During the whole experiment, the two reactors were operated at the temperature of 25 ± 2 °C.

2.2 Building a protective layer on FO membrane

The FO membrane with a self-forming protective layer was prepared by an FO reactor (as illustrated in Fig. S2). Compared with the FST reactor mentioned above, the FO reactor had the same feed solution system, draw solution system except for only putting FO membrane module in the reactor. Whereas, the operating process of the FO reactor was aimed to coat a protective layer

on FO membrane, which was significantly different with the FST reactor for sludge thickening. During the building protective layer process, WAS was firstly pumped into the FO reactor to make the reactor full of the sludge, and then the FO membrane module was continuously operated for 4 days with the draw solution of 0.5 M NaCl solution, and in the meanwhile the sludge concentration of the reactor was kept at 3-4 g/L by circulating WAS in the feed tank and the reactor. After that, a protective layer would be coated on the surface of FO membrane. In order to distinguish the FO membrane before and after building a protective layer, they were denoted as a control FO (C-FO) membrane without a protective layer and a modified FO (M-FO) membrane with a protective layer, respectively.

The using procedure of the M-FO membrane is summarized in Fig. 1. After coating a protective layer, the M-FO membrane can be directly used in the FST reactor for sludge thickening. When it was fouled in one cycle of FST reactor, the deposited foulants and the coated protective layer were removed by in-situ physical cleaning, and then the cleaned membrane was re-coated a protective layer via the same building method. After that, the M-FO membrane was reused in another cycle of the FST reactor.

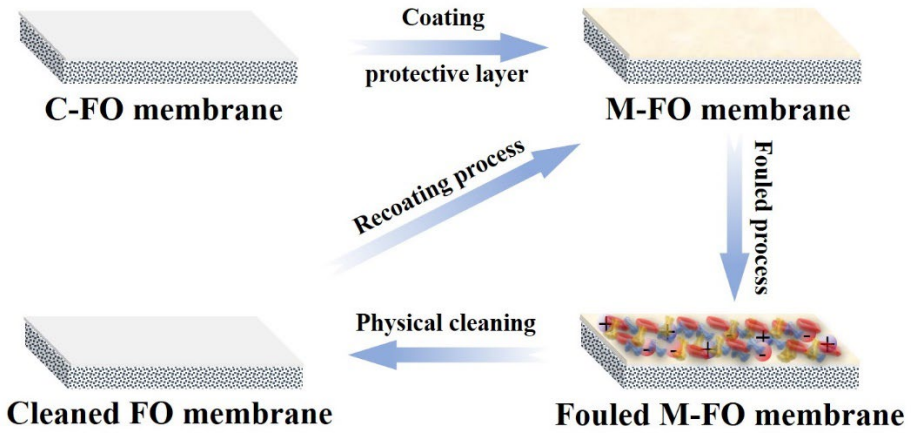

Fig. 1 The coating, fouled, physical cleaning and recoating process of FO membrane.

2.3 Characterization of FO membranes

An FO-Cell system was used to evaluate the water flux (J_w, LMH) and reverse salt flux (J_s, g/(m^2·h)) of both C-FO and M-FO membrane, which were calculated according to Eq. (1) and Eq. (2), respectively. The structure and operating conditions of FO-Cell system have been reported in previous literature [35,36].

$$J_w = \frac{\Delta V}{A_m \Delta t} \quad (1)$$

$$J_s = \frac{C_t V_t - C_0 V_0}{A_m \Delta t} \quad (2)$$

where ΔV is the permeate volume from the feed solution to the draw solution (L); A_m is the active membrane area (m^2); Δt is the operation time (h); C_0 (g/L) and V_0 (L) are the initial concentration and initial volume of the FS, respectively; and C_t (g/L) and V_t (L) are the solute concentration and volume of the FS measured at time t, respectively.

The morphology of both FO membrane surfaces was observed by a Field Emission Scanning Electron Microscope (FE-SEM, Evo18, Carl Zeiss, Germany), and a Solid Surface Zeta Potential Analyzer (SurPASS 3, Anton Paar, Austria) was carried out to assess the changes of membrane surface. The membrane surface hydrophilicity was characterized by the initial contact angle of water using Contact Angle Goniometer (JY-PHb, China). The C-FO and M-FO membrane were tested by an Attenuated Total Reflectance Fourier Transform-infrared Spectrometer (ATR-FTIR, Nicoletis10, Thermo Fisher, USA) in the range of 4000-400 cm^{-1}. In order to analyze the membrane surface topography and roughness, Atomic Force Microscopy (AFM, Multimode-8, Bruker, USA) was performed at room temperature and the scan area of membrane was set at 5 μm × 5 μm. In addition, Confocal Laser Scanning Microscopy (CLSM, LSM 710, Carl Zeiss, Germany) was used to observe the surfaces of the M-FO membrane to investigate the substance composition and distribution of the protective layer, including α-D-glucopyranose and β-D-glucopyranose polysaccharides, proteins

and microorganisms. The three-dimensional CLSM images were obtained via the Image J software, and the biovolume of the substances was calculated by a software of Auto PHLIP-ML (version 1.0). The specific staining method can be found in our previous studies [35,36].

2.4 Performance of FO membranes

The performance of C-FO and M-FO membrane was determined and compared via two identical laboratory-scale FST reactors for thickening WAS. The FST reactors and their operating conditions were described in Section 2.1. In the formal sludge deep thickening process, the MLSS concentration of 50 g/L was regarded as the terminal point. Two consecutive cycles of sludge deep thickening were conducted to compare the performance of both FO membranes. After the MLSS concentration reached 50 g/L for the first time, the thickened sludge was discharged from the reactor and the FO membranes were taken out for physical cleaning. As for the C-FO membrane after physical cleaning, it was put into the FST reactor for the second cycle of thickening WAS. Whereas, the protective layer on the M-FO membrane was firstly removed from FO membrane surface via physical cleaning, and then the M-FO membrane was re-coating a new protective layer with the same procedure described in section 2.2. After that, the M-FO membrane was put into the FST reactor for the second cycle of thickening WAS. It should be pointed out that the physical cleaning of both FO membranes was conducted via osmosis backwashing in the FST reactors, i.e., the feed solution and draw solution were changed to 1.0 M NaCl solution and deionized (DI) water, respectively, and the water flux of both membranes after physical cleaning was determined to evaluate the cleaning efficiency using DI water and 1.0 M NaCl solution as feed solution and draw solution, respectively.

During operating two cycles of both FST reactors, ammonia nitrogen (NH_4^+-N), nitrate

195 nitrogen (NO_3^--N), total phosphorus (TP), total solid (TS), volatile solid (VS), MLSS and mixed
196 liquor volatile suspended solids (MLVSS) were measured according to the Standard methods [37],
197 and total organic carbon (TOC) concentration was determined by a TOC analyzer (TOC-V_{CPH},
198 Shimadzu, Japan). In addition, the fouled FO membranes were analyzed by the in-situ instruments
199 of FE-SEM and CLSM according to the methods described in section 2.3. Furthermore, the foulants
200 on both C-FO and M-FO membrane surface after two consecutive cycles of sludge deep thickening
201 were extracted and divided into reversible and irreversible foulants. The reversible foulants were
202 collected via flushing the surface of FO membranes using the DI water, and then the irreversible
203 foulants were obtained by sonication treatment (50 Hz, 220 V) for the fouled FO membranes for 30
204 min. After that, the extracted reversible and irreversible foulants were diluted with DI water to
205 volume of 100 mL. Subsequently, their total solid (TS) and volatile solid (VS) concentrations were
206 measured.
207
208 **3. Results and discussion**
209 *3.1 Characteristics of FO membrane with protective layer*
210 The surface morphologies of both C-FO and M-FO membranes visualized by SEM, CLSM and
211 FT-IR are illustrated in Fig. 2. The C-FO membrane presented an appearance of a “grid” structure
212 (Fig. 2(a)), while the grid structure was almost disappeared in the M-FO membrane (Fig. 2(d)). The
213 different surface morphology indicated that a protective layer was completely covered on the M-FO
214 membrane surface. From CLSM images (Fig. 2(b) and (e)), the mean thickness of the C-FO and M-
215 FO membrane was 4.0 and 24.5 μm, respectively, which means that the protective layer on the M-
216 FO membrane surface was with an average thickness of 20.5 μm. In addition, the color of cyan,

blue, green and red represented α-D-glucopyranose and β-D-glucopyranose polysaccharides, proteins and microorganisms in CLSM images, respectively. It could be seen from Fig. 2(b) that there was nothing of these four substances on the C-FO membrane surface, whereas the presence of these substances was clearly observed on the M-FO membrane surface and β-D-glucopyranose polysaccharides and microorganisms were the main substances according to their biovolume (see Table S2). The ATR-FTIR (Fig. 1(c)) indicated that the C-FO membrane was characterized by typical absorbance peaks at wavenumber of 1740 cm^{-1} (ester C=O stretching in cellulose triacetate), and 1366, 1214, and 1031 cm^{-1} (C–O stretching in hydroxyl functional group) [38,39]. However, in the spectrum of M-FO membrane, the intensities of these typical absorbance peaks of the C-FO membrane decreased dramatically, and the stronger peak at 1640 cm^{-1} for C=C stretch and a new peak at 1550 cm^{-1} for C-H stretch were found owing to the organic substances in the protective layer (Fig. 2(f)). The above results exactly indicated that a protective layer was successfully built on the M-FO membrane surface, and the polysaccharides and microorganisms were the main composition of the protective layer.

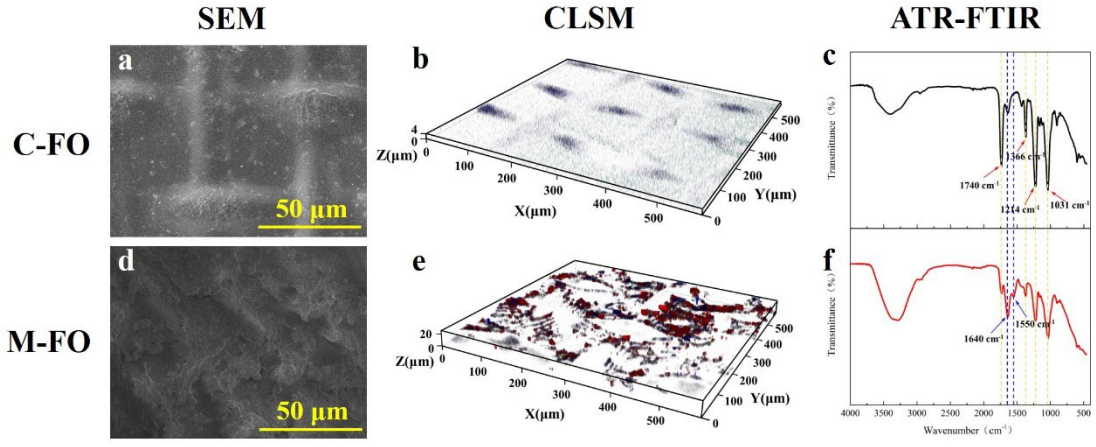

Fig. 2. SEM images (a, d), CLSM images (b, e) and ATR-FTIR spectra (c, f) of both C-FO and M-FO membranes.

The roughness of both C-FO and M-FO membranes was characterized, and their three-

235 dimensional AFM images and the values of average roughness (Ra) are shown in Fig. 3(a). The Ra
236 value of both C-FO and M-FO membranes was 2.17 ± 0.70 and 2.05 ± 0.38 nm, respectively,
237 implying that the protective layer has little effect on the surface roughness of the FO membrane. In
238 addition, the hydrophilicity of both membranes was characterized by contact angle (CA). As shown
239 in Fig. 3(b), the M-FO membrane had a lower CA value (69.8°) than the C-FO membrane (83.4°),
240 indicating the M-FO membrane was indeed more hydrophilic. It is well known that a membrane
241 with smoother and more hydrophilic surface has a higher water flux and a less tendency of fouling.
242 This phenomenon could be due to the presence of some hydrophilic substances in the protective
243 layer [40]. The existence of polysaccharides, a hydrophilic substance [41], in the protective layer
244 has been examined by the results of CLSM (see Fig. 2). Furthermore, the zeta potential values of
245 both membranes at pH values from 4 to 10 were determined, and the results indicated that both
246 membranes had a negative surface charge (Fig. 3(c)). Compared with the C-FO membrane, the M-
247 FO membrane had a higher density of negative charges at pH 4-10. It might be attributed to the
248 presence of polysaccharides in the protective layer, which is a negatively charged organic matter
249 [42,43]. It should be pointed out that the negative charge density of M-FO membrane was obviously
250 higher than that of C-FO membrane at acidic conditions, while the negative charge densities of both
251 membranes became similar when the pH value was larger than 8. It could be attributed to the
252 protective layer fell of the membrane surface at the alkaline condition based on the fact that the
253 alkaline solution is usually used to clean the organic and biological foulants. Since the organic
254 foulants and microorganisms are generally negatively charged at pH value of 7 [41], the M-FO
255 membrane with stronger negative charge on the surface can provide more electrostatic repulsion to
256 improve the antifouling performance of the membrane.

The pure water flux and the reverse salt flux of both membranes are presented in Fig. 3(d). It could be seen that the M-FO membrane had higher water and salt flux compared with the C-FO membrane, and the two membranes had a similar ratio of water flux to reverse salt flux (the J_w/J_s value of both C-FO and M-FO membranes was 0.84 and 0.83, respectively), implying an increase of permeability of FO membrane after coating a protective layer. It might be attributed to the fact that the M-FO membrane was more hydrophilic and had a stronger negative charge surface compared with the C-FO membrane.

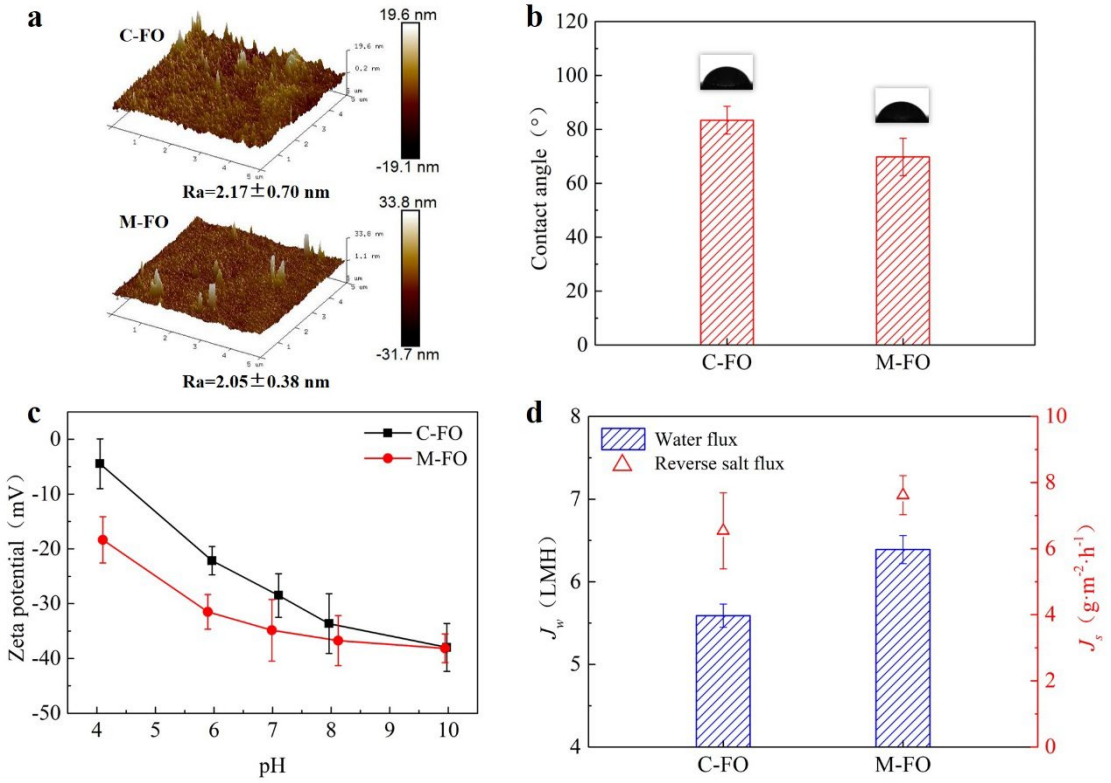

Fig. 3. Properties of both C-FO and M-FO membranes: (a) three-dimensional AFM images; (b) contact angle; (c) zeta potential at pH 4 to 10; (d) pure water flux and reverse salt flux.

3.2 Performance of FO membrane with protective layer during sludge thickening

To verify the feasibility of the fouling control strategy of FO membrane with a protective layer during sludge thickening, the performance of both C-FO and M-FO membranes were investigated

in the FST reactors for thickening WAS. The water flux of both membranes and their sludge thickening efficiency during two operating cycles are summarized in Fig. 4. The water flux of both FO membranes was obviously declined in the two cycles (see Fig. 4(a)), which was consistent with previous literature on FO membrane for sludge thickening [7,16,18,19]. Specifically, the water flux of both membranes had a similar decreasing trend in the first cycle (from 5.12 and 5.32 LMH to 3.49 and 4.03 LMH, respectively), while there was an obvious difference of the flux decline between the two FO membranes in the second cycle. Similar to the first cycle, the water flux of M-FO membrane slowly dropped from 5.07 LMH to 3.95 LMH in the second cycle. In contrast, the water flux of C-FO membrane decreased rapidly from 4.60 LMH to 1.56 LMH in the second cycle. These flux performance results clearly indicated that the M-FO membrane mitigated the flux decline during sludge thickening. It implied that the protective layer effectively alleviated the FO membrane fouling during sludge thickening, which might be owing to the alleviation of irreversible fouling. After Cycle 1, both membranes were physically cleaned to remove the reversible foulants on membrane surfaces. However, the clean efficiency was different between the two FO membranes. As for the C-FO membrane, the flux recovery rate was only 89.8% in Cycle 1 after physical cleaning, indicating some irreversible foulants remaining on the C-FO membrane surface. In this case, more foulants were directly deposited on the C-FO membrane surface and resulting in a significant flux decline. With regard to the M-FO membrane, the protective layer was removed by the physical cleaning after Cycle 1, and the flux recovery rate was almost 100% owing to the protective layer. After that, the protective layer was reloaded on the M-FO membrane surface, and the new foulants would directly interact with the reloaded protective layer instead of the FO membrane surface [44]. Based on the fact that the protective layer was more hydrophilic and more negative charge than the

FO membrane surface, the M-FO membrane was more resistant to foulants than the C-FO membrane, thus leading to alleviating membrane fouling and flux decline. Thanks to the protective layer, as shown in Fig. 4(a), the M-FO membrane successfully concentrated the WAS to 50 g/L in both cycles. However, the C-FO membrane could thicken the WAS to 50 g/L in Cycle 1 but failed in Cycle 2 due to a severe flux decline (see Fig. 4(b)). In addition, NH_4^+-N, NO_3^--N, TP and TOC concentrations in both permeates of the membranes during two cycles of sludge thickening are listed in Table S3. It could be observed that both FO membranes have an excellent retention effect on organic compounds, nitrate and phosphate, and NH_4^+-N, NO_3^--N, TP and TOC concentrations in the permeates were almost no difference between the C-FO and M-FO membrane, which are in accordance with previous reports on the effluent water quality of FO membrane during sludge thickening [7]. The comparison in performance of FST reactor between C-FO and M-FO membrane indicated that the presence of the protective layer on the FO membrane surface had no obvious effect on the retention performance of FO membrane but effectively alleviated flux decline and subsequently enhanced the sludge thickening efficiency.

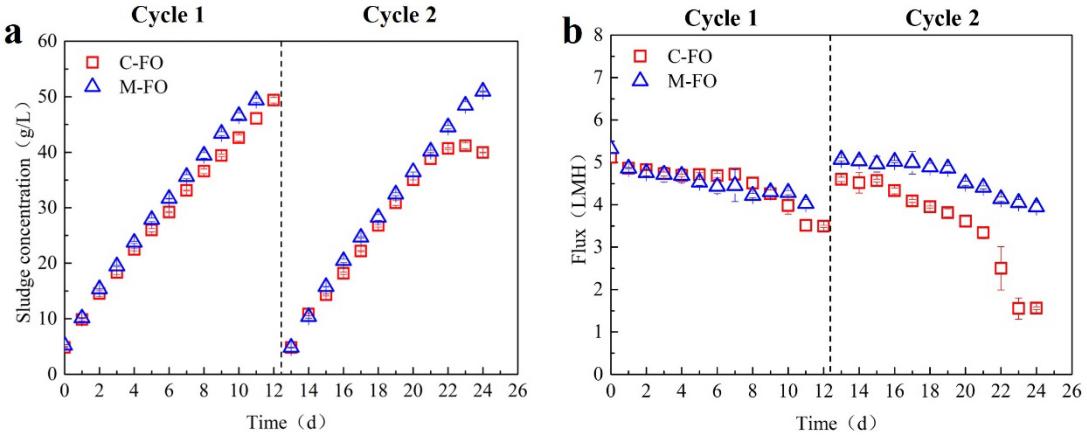

Fig. 4. Sludge thickening efficiency (a) and water flux (b) of both C-FO and M-FO membranes during thickening WAS.

3.3 Fouling behaviors of FO membrane with protective layer during sludge thickening

To further understand the role of protective layer in membrane fouling control, the fouling behaviors of both C-FO and M-FO membranes during sludge thickening were comprehensively analyzed. The composition of the foulants on both membrane surfaces after operating two cycles of sludge thickening is listed in Table 1. The quantities of reversible and irreversible foulants of both membranes were analyzed in the terms of TS and VS concentrations. It could be found from Table 1 that the amount of foulants in terms of TS and VS concentration on the M-FO membrane surface was far less than that on the C-FO membrane surface, indicating the protective layer effectively reducing the deposition of foulants on the membrane surface. In order to further evaluate the mitigation of reversible fouling via the protective layer, the water flux of both C-FO and M-FO membranes before and after physical cleaning were further measured. As shown in Fig. 5, the water flux of both FO membranes decreased obviously after sludge thickening. Specifically, the flux decline rate of both C-FO and M-FO membranes after sludge thickening was 65.5% and 46.3%, respectively, indicating that the fouling of C-FO membrane was more severe than the M-FO membrane, which was consistent with the foulants quantity on the membrane surface (see Table 1). After physical cleaning, the water flux of both C-FO and M-FO membranes recovered by 15.0% and 78.0%, respectively. It implied that the fouling of M-FO membrane was much more reversible compared with the C-FO membrane. The improved reversibility of FO membrane fouling could be attributed to the loading of protective layer. It was well known that membrane fouling caused by direct interaction between the foulants and the membrane surface was more irreversible [44]. The protective layer on the M-FO membrane prevented more foulants from directly interacting with the membrane surface and slowed the accumulation of irreversible foulants on the membrane surface. In addition, the protective layer deposited on the membrane surface would improve the antifouling

performance of FO membrane due to the better hydrophilicity and stronger negative charge of the protective layer, which effectively reduced the deposition of foulants on the M-FO membrane surface (see Table 1). Therefore, the protective layer effectively alleviated the FO membrane fouling via reducing the deposition of foulants and improving the reversibility of membrane fouling.

Table 1 Analyses of the foulants on both C-FO and M-FO membrane surfaces after operating two cycles of sludge thickening [a].

Membrane type	Foulants type	TS (g/m^2)	VS (g/m^2)	VS/TS
C-FO	Reversible foulants	252 ± 38.4	172 ± 35.2	0.68 ± 0.04
	Irreversible foulants	24.7 ± 5.26	6.56 ± 0.19	0.28 ± 0.07
M-FO	Reversible foulants	143 ± 2.48	94.9 ± 0.87	0.66 ± 0.01
	Irreversible foulants	13.4 ± 1.66	4.98 ± 0.23	0.38 ± 0.05

[a] Values are given as mean values ± standard deviation (number of measurements: n = 3).

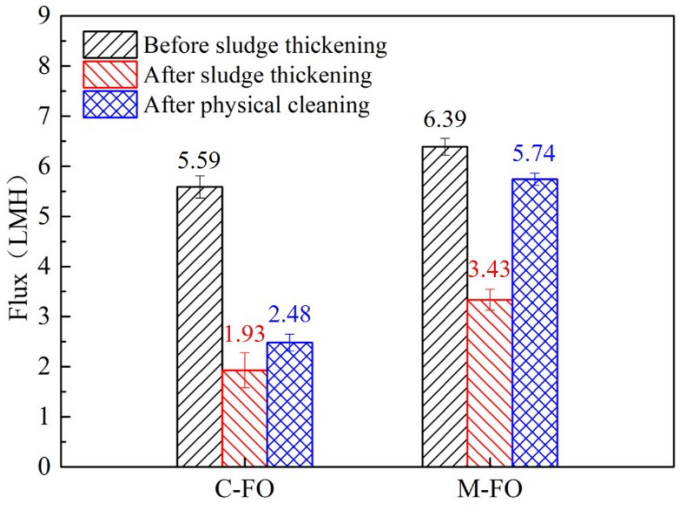

Fig. 5. Water flux of both C-FO and M-FO membranes before and after sludge thickening and after physical cleaning.

In order to investigate the difference of fouling behaviors between the C-FO and M-FO

343 membrane, the surface morphology of two fouled FO membranes was observed by SEM. As shown
344 in Fig. 6, the C-FO membrane was completely covered by foulants (Fig. 6(a)), while the M-FO
345 membrane could vaguely identify the network structure of CTA-FO membrane (Fig. 6(d)). With the
346 increasing of magnification, flakes of foulants could be observed to gather together and adsorbed
347 on the C-FO membrane surface (Fig. 6(b)), but loose foulants aggregates were found on the surface
348 of M-FO membrane (Fig. 6(e)). Based on the fact that the foulants on both FO membrane surfaces
349 were mainly composed of organic matters and biofoulants (i.e., the VS/TS ratio of total foulants was
350 more than 60%), the typical organic foulants and biofoulants including proteins, polysaccharides
351 and microorganisms on both FO membranes were further investigated by the CLSM coupled with
352 multiple fluorescence labeling [35,36]. From Fig. 6(c) and (f), the thickness of fouling layer on both
353 C-FO and M-FO membrane surfaces was 48.0 and 40.5 μm, respectively. The thinner fouling layer
354 on the M-FO membrane surface was consistence of the presence of network structure shown in the
355 SEM image. In addition, the organic foulants and biofoulants on the C-FO membrane surface were
356 obviously denser than that on the C-FO membrane surface (see Fig. 6(c) and (f)). The thicker and
357 denser fouling layer on the membrane surface could be responsible for the severer flux drop of C-
358 FO membrane. For further analyzing the constituents and contents of organic foulants and
359 biofoulants on both FO membrane surfaces, their biovolume was calculated and the related results
360 are summarized in Table S4. From Table S4, the biovolume of all organic foulants and biofoulants
361 on the C-FO membrane was larger than that on the M-FO membrane. Besides, the biovolume of
362 microorganisms was the most widely distributed foulants on the C-FO membrane surface, while the
363 biovolume of microorganisms on the M-FO membrane surface was only 44.0% of that on the C-FO
364 membrane. This phenomenon could be attributed to the protective layer with a stronger negative

charge, which prevented microorganisms with negatively charged [41] from adsorbing on the membrane surface.

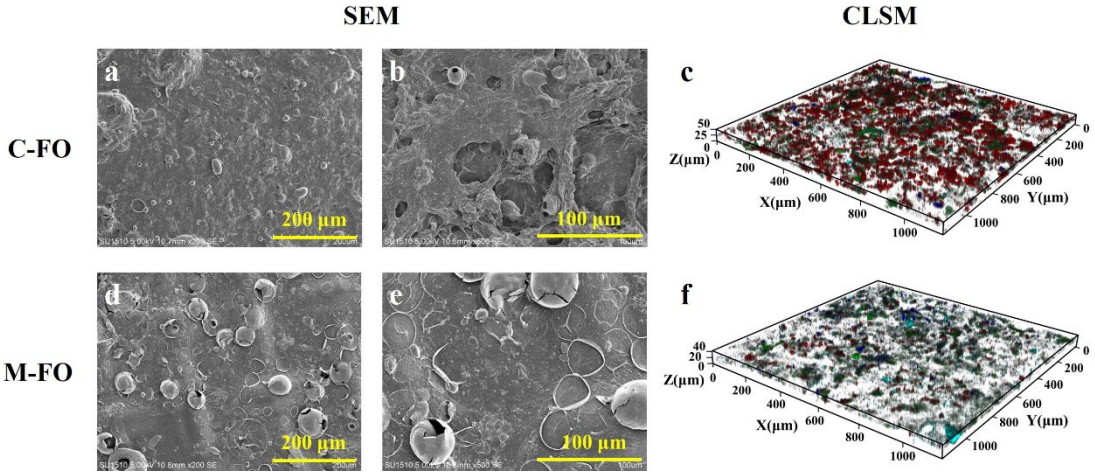

Fig. 6. SEM (a, b, d, e) and CLSM (c, f) images of both C-FO and M-FO membranes after operating two cycles of sludge thickening.

3.4 Implication

According to previous literature [26], the development of FO membrane fouling during sludge thickening could be divided into three stages, i.e., sand-like fouling stage, loose fouling layer stage and dense fouling layer stage. Firstly, inorganic foulants were more likely to deposit on the FO membrane surface and formed a sand-like fouling layer. Secondly, more organic foulants and microorganisms absorbed on the FO membrane surface and thus gradually forming a loose fouling layer. Finally, a large number of foulants deposited and squeezed on the FO membrane surface, which resulted in the formation of a dense fouling layer. Owing to the slight fouling at both Stage 1 and Stage 2, there was no obvious flux decline, whereas the flux of FO membrane decreased significantly at Stage 3 owing to subsequent foulants squeezing the former foulants already on the membrane surface. In this study, the FO membrane with a protective layer had a thinner fouling layer and less foulants after two cycles of sludge thickening, indicating that the protective layer

played a positive role in the third stage of membrane fouling (see Fig. 7). It could be attributed to the fact that the protective layer apparently improved the hydrophilicity and negative charge of the membrane surface, which effectively slowed down the deposition of subsequent organic matter and microorganisms. In addition, the loose protective layer had an excellent support effect, which not only avoided the mutual extrusion of subsequent foulants but also alleviated the deposition of irreversible foulants. Compared with the coating layer prepared by chemical method [30], no chemicals were consumed in the preparation process of the protective layer and physical cleaning was enough for decoating the protective layer in our study. The coating and decoating process of the protective layer reported in this study is economical, environment-friendly and potential. It should be pointed out that the thickness and properties of protective layer can influence the effect of mitigating membrane fouling, which need to be further studied in order to perfect the control method on FO membrane fouling via a protective layer.

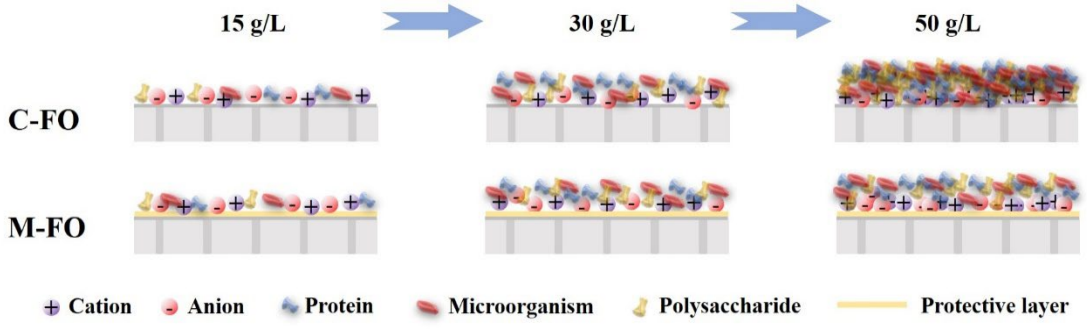

Fig. 7 Schematic diagram of fouling mechanisms of both C-FO and M-FO membranes.

4. Conclusions

In this study, a novel strategy of a self-forming protective layer was performed to mitigate FO membrane fouling during sludge thickening. The protective layer was coated on the FO membrane surface via a short-term operation of FO process with activated sludge as feed solution. The

protective layer had no negative effect on the permeability of membrane, and the presence of protective layer made the FO membrane more hydrophilic and more negatively charged. Compared with the C-FO membrane, the M-FO membrane with a protective layer had a better sludge thickening efficiency and a lower flux declining rate during sludge thickening. After two cycle of sludge thickening, owing to the presence of protective layer, there were less foulants, especially biofoulants, deposited on the M-FO membrane, and the fouling reversibility of FO membrane was obviously improved. The alleviation of FO membrane fouling via the protective layer was attributed to slow the accumulation of irreversible foulants on the membrane surface and improve the antifouling performance of membrane surface through enhancing the hydrophilicity and negative charge.

CRediT author statement

Xiawen Yi: Data curation, Formal analysis, Investigation, Writing – original draft. Kang Chen: Supervision, Writing – original draft. Ming Xie: Conceptualization, Writing – review & editing. Pin Zhao: Investigation, Writing – original draft. Weilong Song: Methodology, Supervision. Xinhua Wang: Conceptualization, Supervision, Writing – review & editing, Funding acquisition.

Declaration of competing interest

The authors declare that they have no known competing financial interests or personal relationships that could have appeared to influence the work reported in this paper.

Acknowledgements

This work was supported by the National Natural Science Foundation of China [grant number 51978312]; the Postgraduate Research & Practice Innovation Program of Jiangsu Provence [grant

423 number KYCX22_2383]; and the Program to Cultivate Middle-aged and Young Science Leaders of
424 Colleges and Universities of Jiangsu Province.

425 **Appendix A. Supplementary data**

426 Supplementary data to this article can be found online.

427 **References**

428 [1] M.L. Christensen, K. Keiding, P.H. Nielsen, M.K. Jorgensen, Dewatering in biological
429 wastewater treatment: a review, Water Res. 82 (2015) 14-24.

430 [2] B. Wu, X. Dai, X. Chai, Critical review on dewatering of sewage sludge: influential mechanism,
431 conditioning technologies and implications to sludge reutilizations, Water Res. 180 (2020)
432 115912.

433 [3] M. Schnell, T. Horst, P. Quicker, Thermal treatment of sewage sludge in Germany: a review, J.
434 Environ. Manage. 263 (2020) 110367.

435 [4] Ministry of Housing and Urban-Rural Development of the People's Republic of China,
436 Statistical Yearbook of Urban and Rural Construction in China (2020).

437 [5] B. Cao, T. Zhang, W. Zhang, D. Wang, Enhanced technology based for sewage sludge deep
438 dewatering: a critical review, Water Res. 189 (2021) 116650.

439 [6] N.C. Nguyen, S.S. Chen, H.Y. Yang, N.T. Hau, Application of forward osmosis on dewatering
440 of high nutrient sludge, Bioresour. Technol. 132 (2013) 224-229.

441 [7] X. Yi, H. Zhong, M. Xie, X. Wang, A novel forward osmosis reactor assisted with microfiltration
442 for deep thickening waste activated sludge: performance and implication, Water Res. 195 (2021)
443 116998.

444 [8] H. Yuan, N. Zhu, F. Song, Dewaterability characteristics of sludge conditioned with surfactants

445 pretreatment by electrolysis, Bioresour. Technol. 102 (2011) 2308-2315.
446 [9] M.S. Kim, K.M. Lee, H.E. Kim, H.J. Lee, C. Lee, C. Lee, Disintegration of Waste Activated
447 Sludge by Thermally-Activated Persulfates for Enhanced Dewaterability, Environ. Sci. Tech.
448 50 (2016) 7106-7115.
449 [10] W. Yu, J. Yang, Y. Shi, J. Song, Y. Shi, J. Xiao, C. Li, X. Xu, S. He, S. Liang, X. Wu, J. Hu,
450 Roles of iron species and pH optimization on sewage sludge conditioning with Fenton's reagent
451 and lime, Water Res. 95 (2016) 124-133.
452 [11] X. Wang, Z. Wu, Z. Wang, X. Du, J. Hua, Membrane fouling mechanisms in the process of
453 using flat-sheet membrane for simultaneous thickening and digestion of activated sludge, Sep.
454 Purif. Technol. 63 (2008) 676-683.
455 [12] Z. Wang, Z. Wu, J. Hua, X. Wang, X. Du, H. Hua, Application of flat-sheet membrane to
456 thickening and digestion of waste activated sludge (WAS), J. Hazard. Mater. 154 (2008) 535-
457 542.
458 [13] X. Wang, Z. Wu, Z. Wang, X. Yin, X. Du, Floc destruction and its impact on dewatering
459 properties in the process of using flat-sheet membrane for simultaneous thickening and
460 digestion of waste activated sludge, Bioresour. Technol. 100 (2009) 1937-1942.
461 [14] Z. Wu, X. Wang, Z. Wang, X. Du, Identification of sustainable flux in the process of using flat-
462 sheet membrane for simultaneous thickening and digestion of waste activated sludge, J. Hazard.
463 Mater. 162 (2009) 1397-1403.
464 [15] H.G. Kim, H.N. Jang, H.M. Kim, D.S. Lee, T.H. Chung, Effects of the sludge reduction system
465 in MBR on the membrane permeability, Desalination 250 (2010) 601-604.
466 [16] H. Zhu, L. Zhang, X. Wen, X. Huang, Feasibility of applying forward osmosis to the

467 simultaneous thickening, digestion, and direct dewatering of waste activated sludge, Bioresour.
468 Technol. 113 (2012) 207-213.
469 [17] H.G. Kim, T.H. Chung, Performance of the sludge thickening and reduction at various factors
470 in a pilot-scale MBR, Sep. Purif. Technol. 104 (2013) 297-306.
471 [18] N.T. Hau, S.S. Chen, N.C. Nguyen, K.Z. Huang, H.H. Ngo, W. Guo, Exploration of EDTA
472 sodium salt as novel draw solution in forward osmosis process for dewatering of high nutrient
473 sludge, J. Membr. Sci. 455 (2014) 305-311.
474 [19] N.C. Nguyen, H.T. Nguyen, S.S. Chen, N.T. Nguyen, C.W. Li, Application of forward osmosis
475 (FO) under ultrasonication on sludge thickening of waste activated sludge, Water Sci. Technol.
476 72 (2015)1301-1307.
477 [20] E.R. Cornelissen, D. Harmsen, K.F. Dekorte, C.J. Ruiken, J.J. Qin, H. Oo, L.P. Wessels,
478 Membrane fouling and process performance of forward osmosis membranes on activated
479 sludge, J. Membr. Sci. 319 (2008) 158-168.
480 [21] X. Zhang, Z. Ning, D.K. Wang, J.C. Diniz da Costa, Processing municipal wastewaters by
481 forward osmosis using CTA membrane, J. Membr. Sci. 468 (2014) 269-275.
482 [22] Y. Sun, J. Tian, Z. Zhao, W. Shi, D. Liu, F. Cui, Membrane fouling of forward osmosis (FO)
483 membrane for municipal wastewater treatment: A comparison between direct FO and OMBR,
484 Water Res. 104 (2016) 330-339.
485 [23] X. Wang, C. Wang, C.Y. Tang, T. Hu, X. Li, Y. Ren, Development of a novel anaerobic
486 membrane bioreactor simultaneously integrating microfiltration and forward osmosis
487 membranes for low-strength wastewater treatment, J. Membr. Sci. 527 (2017) 1-7.
488 [24] H. Wang, X. Wang, F. Meng, X. Li, Y. Ren, Q. She, Effect of driving force on the performance

489 of anaerobic osmotic membrane bioreactors: New insight into enhancing water flux of FO
490 membrane via controlling driving force in a two-stage pattern, J. Membr. Sci. 569 (2019) 41-
491 47.
492 [25] N.D. Viet, S.J. Im, A. Jang, Characterization and control of membrane fouling during
493 dewatering of activated sludge using a thin film composite forward osmosis membrane, J.
494 Hazard. Mater. 396 (2020) 122736.
495 [26] X. Yi, H. Zhong, M. Xie, P. Zhao, W. Song, X. Wang, Novel insights on fouling mechanism of
496 forward osmosis membrane during deep thickening waste activated sludge, J. Membr. Sci. 660
497 (2022) 120894.
498 [27] F. Sun, D. Lu, J.S. Ho, T.H. Chong, Y. Zhou, Mitigation of membrane fouling in a seawater-
499 driven forward osmosis system for waste activated sludge thickening, J. Clean. Prod. 241 (2019)
500 118317.
501 [28] D.Y.F. Ng, B. Wu, Y. Chen, Z. Dong, R. Wang, A novel thin film composite hollow fiber
502 osmotic membrane with one-step prepared dual-layer substrate for sludge thickening, J. Membr.
503 Sci. 575 (2019) 98-108.
504 [29] M. Yan, M. Shao, J. Li, N. Jiang, Y. Hu, W. Zeng, M. Huang, Antifouling forward osmosis
505 membranes by ε-polylysine mediated molecular grafting for printing and dyeing wastewater:
506 Preparation, characterization, and performance, J. Membr. Sci. 668 (2023) 121288.
507 [30] S. Li, H. Meng, H. Wang, J.S. Vrouwenvelder, Z. Li, A sacrificial protective layer as fouling
508 control strategy for nanofiltration in water treatment. Water Res. 219 (2022) 118554.
509 [31] C. Ba, D.A. Ladner, J. Economy, Using polyelectrolyte coatings to improve fouling resistance
510 of a positively charged nanofiltration membrane, J. Membr. Sci. 347 (2010) 250-259.

511 [32] M. Son, W. Yang, S.S. Bucs, M.F. Nava-Ocampo, J.S. Vrouwenvelder, B.E. Logan,
512 Polyelectrolyte-Based Sacrificial Protective Layer for Fouling Control in Reverse Osmosis
513 Desalination. Environ, Sci. Tech. Let. 5 (2018) 584-590.
514 [33] X. Zhu, H. Liang, X. Tang, L. Bai, X. Zhang, Z. Gan, X. Cheng, X. Luo, D. Xu, G. Li,
515 Supramolecular-Based Regenerable Coating Layer of a Thin-Film Composite Nanofiltration
516 Membrane for Simultaneously Enhanced Desalination and Antifouling Properties, ACS Appl.
517 Mater. Inter. 11 (2019) 21137-21149.
518 [34] M.F. Nava-Ocampo, S.S. Bucs, A.S.F. Farinha, M. Son, B.E. Logan, J.S. Vrouwenvelder,
519 Sacrificial coating development for biofouling control in membrane systems, Desalination 496
520 (2020) 114650.
521 [35] B. Yuan, X. Wang, C.Y. Tang, X. Li, G. Yu, In situ observation of the growth of biofouling layer
522 in osmotic membrane bioreactors by multiple fluorescence labeling and confocal laser
523 scanning microscopy, Water Res. 75 (2015) 188-200.
524 [36] X. Wang, Y. Zhao, B. Yuan, Z. Wang, X. Li, Y. Ren, Comparison of biofouling mechanisms
525 between cellulose triacetate (CTA) and thin-film composite (TFC) polyamide forward osmosis
526 membranes in osmotic membrane bioreactors, Bioresour. Technol. 202 (2016) 50-58.
527 [37] Chinese NEPA, Water and Wastewater Monitoring Methods, third ed., Chinese Environmental
528 Science Publishing House, Beijing, 2002.
529 [38] W. Luo, M. Xie, F.I. Hai, W.E. Price, L.D. Nghiem, Biodegradation of cellulose triacetate and
530 polyamide forward osmosis membranes in an activated sludge bioreactor: Observations and
531 implications, J. Membr. Sci. 510 (2016) 284-292.
532 [39] J. Ding, G.V. Sarrigani, H.J. Khan, H. Yang, N.A. Sohimi, N.Z. Izzati Sukhairul Zaman, X.

533 Zhong, A. Mai-Prochnow, D.K. Wang, Designing Hydrogel-Modified Cellulose Triacetate
534 Membranes with High Flux and Solute Selectivity for Forward Osmosis, Ind. Eng. Chem. Res.
535 59 (2020) 20845-20853.
536 [40] J.T. Arena, B. McCloskey, B.D. Freeman, J.R. McCutcheon, Surface modification of thin film
537 composite membrane support layers with polydopamine: Enabling use of reverse osmosis
538 membranes in pressure retarded osmosis, J. Membr. Sci. 375 (2011) 55-62.
539 [41] H. Lin, M. Zhang, F. Wang, F. Meng, B.Q. Liao, H. Hong, J. Chen, W. Gao, A critical review
540 of extracellular polymeric substances (EPSs) in membrane bioreactors: Characteristics, roles
541 in membrane fouling and control strategies, J. Membr. Sci. 460 (2014) 110-125.
542 [42] Z. Li, P. Lu, D. Zhang, G. Chen, S. Zeng, Q. He, Population balance modeling of activated
543 sludge flocculation: Investigating the influence of Extracellular Polymeric Substances (EPS)
544 content and zeta potential on flocculation dynamics, Sep. Purif. Technol. 162 (2016) 91-100.
545 [43] C. Chen, T. Zhang, L. Lv, Y. Chen, W. Tang, S. Tang, Destroying the structure of extracellular
546 polymeric substance to improve the dewatering performance of waste activated sludge by ionic
547 liquid, Water Res. 199 (2021) 117161.
548 [44] C. Zhang, Q. Bao, H. Wu, M. Shao, X. Wang, Q. Xu, Impact of polysaccharide and protein
549 interactions on membrane fouling: Particle deposition and layer formation, Chemosphere. 296
550 (2022) 134056.
551